Science on Form: Proceedings of the Second International Symposium for Science on Form,
Editor: S. Ishizaka, pp. 199–217.

3D SHAPE ANALYSIS OF SOLIDS VIA THE DISCRETE FOURIER SINE(COSINE) TRANSFORMATION

Toshiharu SHIBATA and Kenji YAMAGUCHI

Department of Applied Chemistry, Faculty of Engineering, Hokkaido University, Sapporo 060, Japan

Key words: Fourier sine coefficient, Estimations of surface area and volume

Abstract. Among many orthogonal transformations, the discrete Fourier method is focused because of characteristics as

i) Well reproducibility not only at prescribed N points from contours but over their intervals,

ii) Significant designation and operationability of coefficients.

In succession of considerations on the above characteristics, salient silhouettes of solid samples under stepwise rotations are analyzed three-dimensionally. From the results, surface area, volume, shape characteristics such as elongation, flatness and so on, are correlated with a set of the sine coefficients and the shape samples are located in a characteristic coordinate space.

INTRODUCTION

The Fourier methods have been developed solely or in cooperation with such fields as pattern recognitions and information analyses since 1960's. Schwalcz & Shane (1969) applied it in approximate finite series to an analysis of grain projection and they especially interested in its equivalent radius related to the average base point. Ehrlich & Weinberg (1970) analysed shapes of geological quartzes.

Particle or particulate shapes have been also analysed in its silhouettes by Fourier series techniques to obtain the qualitative characteristics for physical properties. Meloy (1977) proceeded with the many research works on powder or particulate systems extensively since 1969. Beddow (1975) also widely refined the analysis and extended it to many applications. Although the order is inverted, historically, Cosgriff (1960) suggested availability of the Fourier descriptors in the first pioneering work ("Identification of Shape", Ohio State Univ. Res. Foundation, Columbus, Rep. 820-11, ASTIA AD 254792). Zahn & Roskies (1972) also systematized the Fourier method for character or shape recognitions.

This paper was presented at The Second International Symposium for Science on Form (October 19th–21st, 1988 at the University of Tsukuba, Japan).

Many research works mentioned above and successive ones have been concerned with the analysis (discrete or continuous) which may be either the sine-cosine transformation or the cosine (sine) transformation with phase angles and their spectral mode has been discussed. In a view of methodrogies, an exceptional but interesting discrete cosine transformation, DCT of which an argument is defined in a different manner was discussed by Ahmed *et al.* (1974). They used an odd index argument and compared the performance with other methods such as the Karhunen-Loeve (KLT), the Walsh-Hadamard and the Haar as well as the Fourier expansion. The theory was commented by Shanmugam (1975) that the transformation is asymptotically equivalent to the KLT. The DCT may be characteristic as for no phase angle and the arguments with the odd index. Jain (1979) also introduced some discrete sine transformations which he considered to a sinusoidal family of unitary transforms. He applied the transformations to two dimensional image processings and pursuited the computational performances. The phase angles have rather random nature, so its has been said that they may be less important than amplitude coefficients. However, Oppenheim & Lim (1981) showed that more importance of the phase effects in cases of signal processings and synthesizings than spectral magnitude. Thus, no phase angle by proper logics may be desirable for better classifications, reconstructions and information extractions for shapes. As for the no phase angle, Luerkens, Beddow & Vetter (1982a, b) succeeded to eliminate it with the size and shape descriptors starting from the usual expressions. Their method requires the expence of the substantial procedures at the inverse transformation (Luerkens *et al.*: 1982a).

In a present report, a simplified discrete Fourier transformation method so-called a half-range method, is treated. The method uses either sine or cosine function with no aid of phase angles. And both functions also available at special requests, for example, in a case of comparison and transition from/to the traditional. The present analysis should be defined in an open interval $(0, 2\pi)$ instead of a closed one $[0, 2\pi]$ and therefore two end points 0 and 2π are regarded to special. Consequently, the present sine or cosine transformation does use no phase angle which will make many following analyses simpler without loss of their shape informations in the descriptors except only an initial starting point, $t=0$, where the true value should be noted as an additional characteristics if only either use.

1. THE DISCRETE FOURIER ANALYSIS FOR PARTICLE SHAPE CONTOURS

1.1 Informations contained in Fourier sine and cosine coefficients

It is well known that we have to use sine-cosine functions in a Fourier analysis of an arbitrary continuous univalent function which is classified to neither odd nor even. Of course, if a function by which a particle contour is described, is evenly symmetric, then the cosine expansion is available. On the other side, although in the contour analysis we usually could not carry out with only sine series, its tangent curve will be described with it in a case of its odd nature. As a matter of fact, in particurate analyses, it is usual that the cosine expansion has been used under an axi-symmetrically oriented particurate position, they are sometimes duplicated to symmetrical bodies of revolution, such as sphere, ellipsoids and so on. Rhombi or squares were also compared with the silhouette of particles.

Now, when symmetric patterns are rotated around a certain point, i.e. a center of gravity, then Fourier cosine informations are changed or transformed into a sequence of the sine informations degree by degree and vice versa. This may suggest that the informations have interchangeability. Besides between sine and cosine coefficients, an even or odd characteristic of trigonometric function is not fixed in itself but there is some shiftability in contrast to other not-interchangeable functions such as a linear (odd) and a parabola (even) and so on. Now, let us examine a function which is transformed,

—a function is represented by discrete points but it has periodic natures—

—it has an even symmetry—

Then, we get transformed functional sequences of which components are as follow,

$$\{A_k \cos(2\pi\, kt/2N)\},\ k=1, 2, \ldots, N-1$$

In the expression, $2N$ is a number of discrete sample points and 'k' is an integer index.

Now, when we look at the sequence, we may regard it as an even part from a certain sequence, $A_k{}' \cos(\pi k't/2N)$. For the sake of sameness between symmetry and even indices we have lost the effect of odd indices as well as an odd symmetry can have odd indices.

$$\begin{aligned} & B_k \sin(\pi t(2k+1)/2N) \\ &= (B_k{}' \cos(\pi t/2N)) \sin(2\pi k't/2N) + B_k{}' \cos(2\pi k't/2N) \sin(\pi t/2N) \\ &= B_k{}'' \sin(2\pi k't/2N) + 0 \end{aligned} \tag{1}$$

where $B_k{}''$ is a new constant and this does not depend on its parity and the last term in the second equation should be eliminated because of its even assumption. The above relation shows that the two sets of the Fourier coefficients with the suffix k from arguments $2k$ and $2k+1$ are compatible. It is suggested that the suffix is not necessary to be integer but half integers such as $k=0.5, 1.5, ..$ among $k=0, 1, ...$ After this we can use the numeral $m\pi$ instead of 2π. Here, the parameter 'm' will take one for the simplicity and its enough.

Now we refer the identity equation for an arbitrary function $f(t)$,

$$f(t) = \{f(t) + f(-t)\}/2 + \{f(t) - f(-t)\}/2 \tag{2}$$

where the first term in the right side is an even function and the second is an odd one. The equation does not show a substantial decomposition. However when we can have defined an odd function and we reduce it from the original $f(t)$, then we always get a corresponding even function and vice versa.

1.2 Presentation of the simplified discrete Fourier expansion

Form the above considerations, a next set is possible.

$$f_{oe}(t) = \frac{A_0}{2} + \sum_{k=1}^{N-1}{}' A_k \cos\left(\frac{\pi kt}{N}\right) + \sum_{k=1}^{N-1}{}' B_k \sin\left(\frac{\pi kt}{N}\right) + \frac{A_N}{2}\cos(Nt)(0 < t < 2\pi) \tag{3}$$

$$f_e(t) = 2\sum_{k=1}^{N-1}{}' A_k \cos\left(\frac{\pi kt}{N}\right) \qquad (0 < t < 2\pi) \tag{4}$$

$$f_o(t) = 2\sum_{k=1}^{N-1}{}' B_k \sin\left(\frac{\pi kt}{N}\right) \qquad (0 < t < 2\pi) \tag{5}$$

where two coefficients A and B are defined by

$$A_k = \frac{1}{N}\sum_{k=1}^{N-1}{}' f_i(t) \cos\left(\frac{\pi kt}{N}\right) \tag{6}$$

$$B_k = \frac{1}{N}\sum_{k=1}^{N-1}{}' f_i(t) \sin\left(\frac{\pi kt}{N}\right) \tag{7}$$

$$k = 0, 1, \dots, N-1, \; i = \text{oe, o, e}.$$

These equations will be listed later, in refined forms together with $f(t)$=const. The equations do almost correspond to the previous except of 'i' and absence of a numeral 2 in the term $\pi kt/N$, where N is a number of Fourier samples. Now, with the use of an open interval $(0, 2\pi)$ for t, we can find the equivalent relations among the set as

$$f_{oe}(t) = f_e(t) = f_o(t) = f(t) \qquad (0 < t < 2\pi). \tag{8}$$

As for the subscripts, o, e and oe are odd, even and neither odd nor even, respectively, and finally they will no need to be distinguished. The present sine series, $f_o(t)$, is not necessary to restrict to the odd characteristic because the even nature appears in its odd subseries, crosswisely and vice versa.

2. NUMERICAL EXAMPLES AND SOME CHARACTERISTICS BY THE HALF-RANGE EXPANSION

First of all, let us take up an example of a closed analytical polygon as in Fig. 1. A circle of a broken curve is by an equivalent diameter and a symmetrical chained pattern is from a skeletal extract so-called, cosine components of the hexagon and a couple of trefoils comes from its details (sine components). Here, we illustrate the inversion in terms of the two series sums (either of sine or cosine coefficients). As the coefficients with the even suffix are quite same, and the odds are crosswisely compared with the traditional ones as in Fig. 2. As known from the definition of sine function, the inverted $f(t)$ with the sine coefficients has always zero only at the initial start point t=0 in spite of the non-zero of $f(0)$. But it is not fatal. If necessary to avoid this, a vertical translation of the abcissa may be useful for the elimination of the initial discrepancy (Fig. 3), resulted to a kind of the epithelium. On a typical nature of Fourier coefficients, the first cosine coefficient is directly related with the

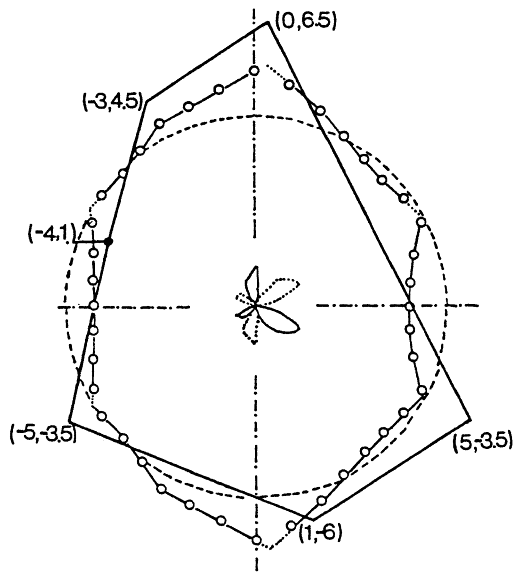

Fig. 1. A test pattern—hexagon—.

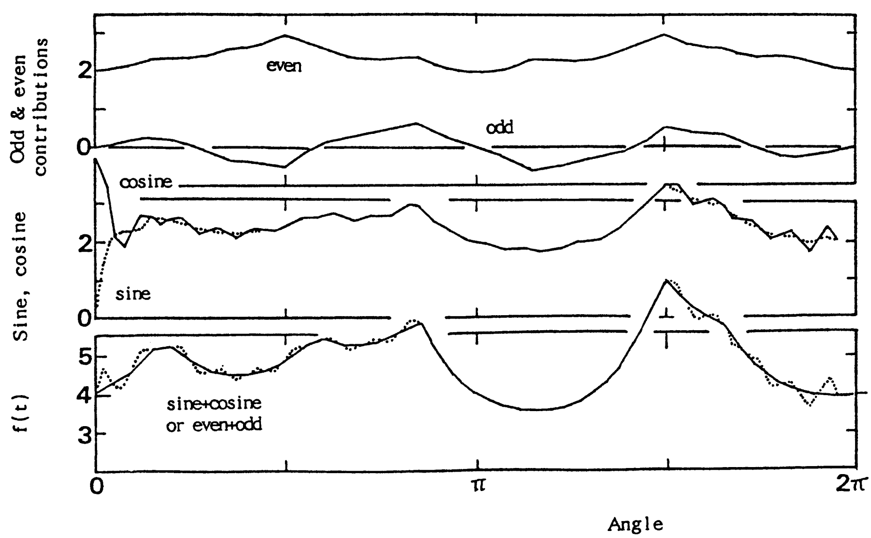

Fig. 2. Inversed results for hexagon (original).

size of shape as known from Eq. 6 with $k=0$. Such a nature also approximately appears in the first nonzero-sine coefficient with $k=1$. Thus a selection of the sine or the cosine coefficients may not be absolutely deterministic because of the shiftability. As for the shift of informations, we have a horizontal rotation of shapes. Figure 4 is

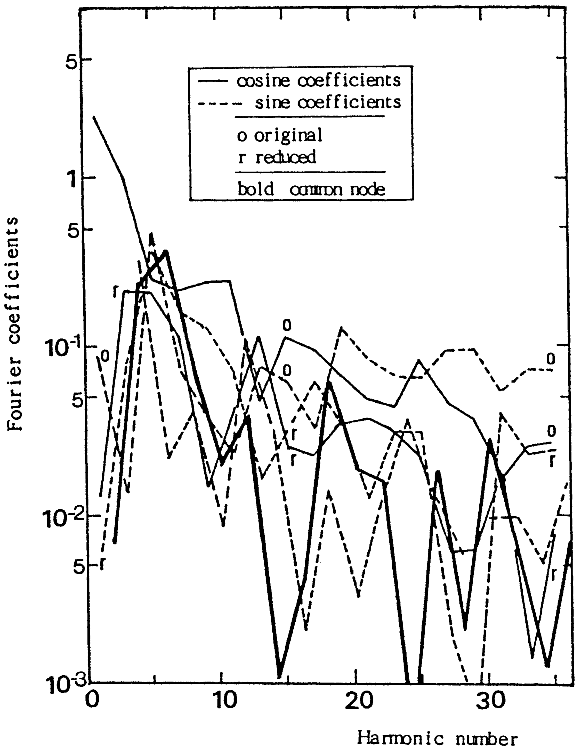

Fig. 3. Behavior of coefficients for the hexagon—various reductions keep the same node points—.

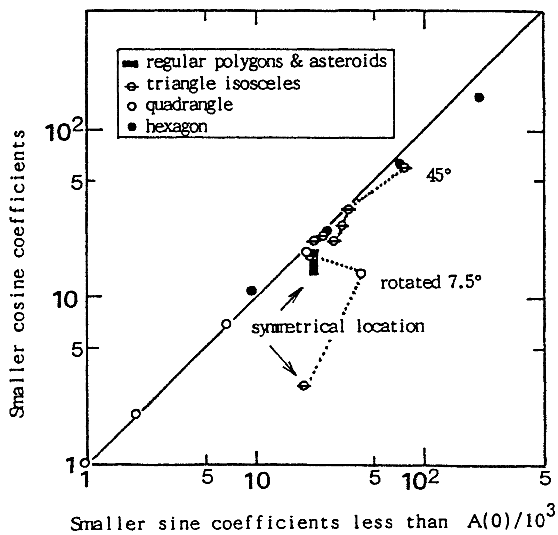

Fig. 4. Comparison of two smaller coefficients—symmetrical location concentrates informations into sine coefficients—.

the result of the rotation and it tells that a symmetrical allocation of shapes extracts the more significant coefficients into the sine sets and in the linear way related to the Fourier sampling (Fig. 5).

As for the inversion of shapes, original points on the contour will be always regenerated correctly. However, in the usual discrete Fourier analysis, only the original sampling points are defined and other points such as intermediates are regarded as zero. The present method has an objection to this (Fig. 6).

Figure 7 shows states of erroneous differences at the middle-point where the largest error will appear. Here, the lines named to the maximum errors lay near the initial region in a concentrated way. Increasing the sampling points diminishes the errors more efficiently in the inversion with the sine coefficients.

In order to examine constructive precisions, the initial hexagon was treated with much more sampling points of 640, and the major coefficients were counted and were inverse-transformed. The result shows that the major from the more sampling is not always superior than no cut-off minor (Fig. 8).

Last of the present discrete transformation, three kinds of sums for the sine coefficients $B(2k+1)$, themselves, squared and cubic, are examined with increasing the number of Fourier sampling. It is shown that differences of shapes can be eliminated by the normalization with the size parameter $A(0)$ and the sampling

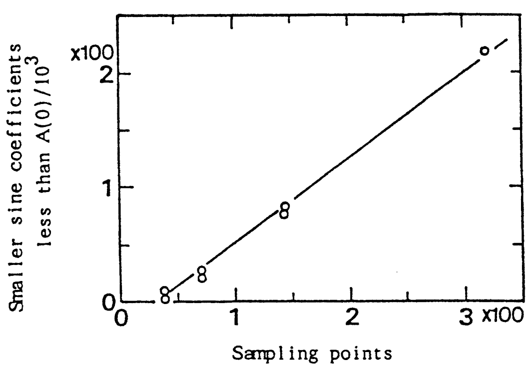

Fig. 5. Linear increase of smaller sine coefficients with the sampling points—polygons, triangles, penta-, hexa-gons etc.—.

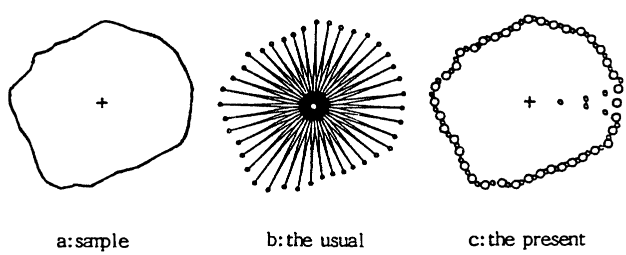

Fig. 6. Comparison between the present and the usual.

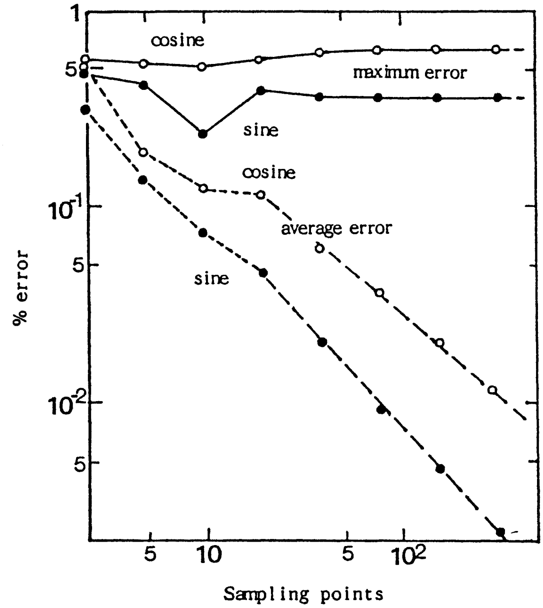

Fig. 7. Effect of a number of sampling points on interpolative errors.

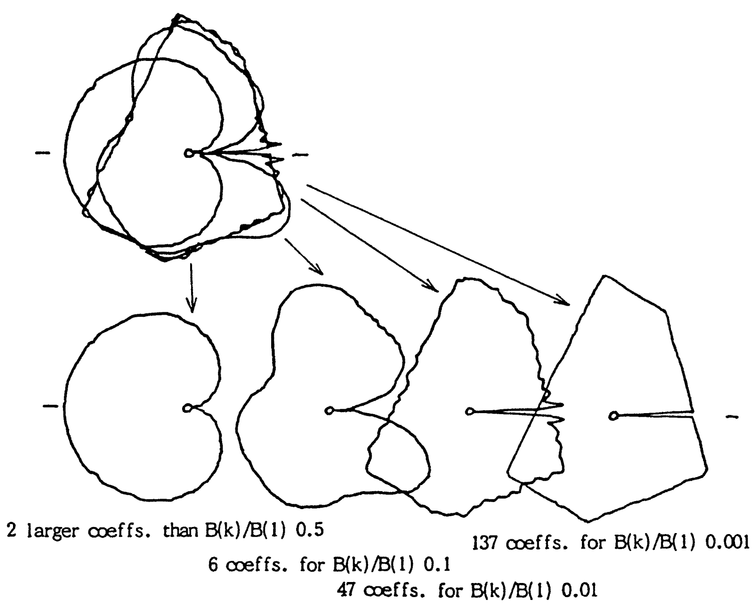

Fig. 8. Cut-off of smaller coefficients, from 640 Fourier sampling points.

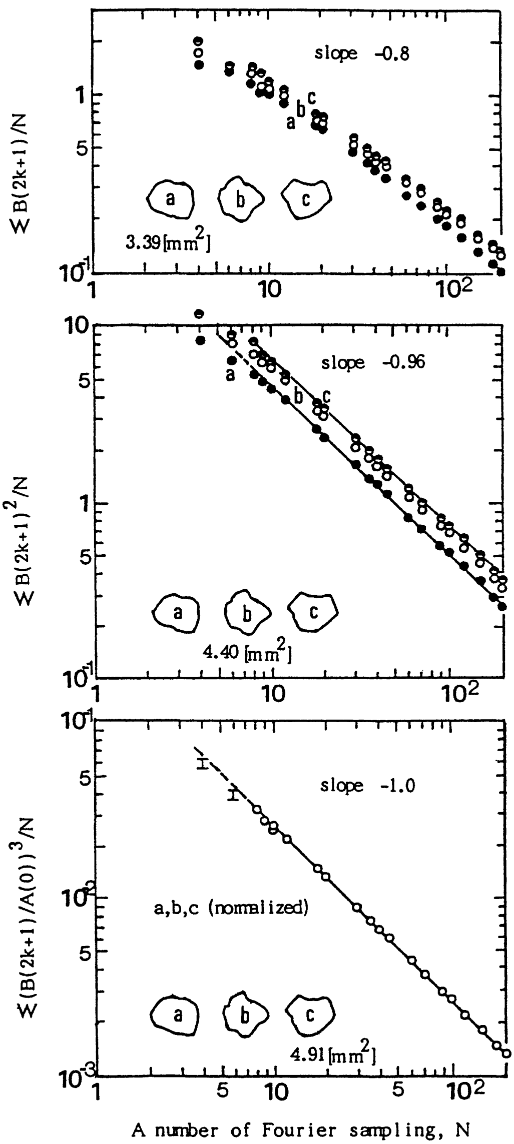

$$A_k = \frac{1}{N}\sum_{t=0}^{N-1} f(t)\cos\frac{\pi k t}{N}, \quad \boxed{B_k = \frac{1}{N}\sum_{t=0}^{N-1} f(t)\sin\frac{\pi k t}{N}}$$

$$k = 0, 1, 2, 3, \cdots, N-1, (N)$$

$$f(t) = \frac{A_0}{2} + \sum_{k=1}^{N-1}\left(A_k\cos\frac{\pi k t}{N} + B_k\sin\frac{\pi k t}{N}\right) + \frac{A_N}{2}\cos\pi t$$

$$= 2\left(\frac{A_0 + A_N\cos\pi t}{2} + \sum_{k=1}^{N-1} A_k\cos\frac{\pi k t}{N}\right) 2^{-\delta_{0t}}$$

$$= \left(\frac{A_0 + A_N}{2} + \sum_{k=1}^{N-1} A_k\right)\delta_{0t} + 2\sum_{k=1}^{N-1} B_k\sin\frac{\pi k t}{N}$$

$\delta_{0t} = 1$ at $t = 0$ and $\delta_{0t} = 0$ at $t \neq 0$

$$B^{\circ}_{2k+1} = \frac{c/N}{\tan\frac{(2k+1)\pi}{2N}} \quad \text{for } f(t) = c \text{ ; constant}$$

Fig. 9. Stable relations between sums of powered sequences and a number of Fourier samplings.

points more than forty will result to stable alternation of the sums, which will be useful in following main analyses (Fig. 9).

3. EXPERIMENTAL PREPARATION

Every closed contour of image planes is digitized into one valued distance sequence with incremental angle step and a number of the terms of the sequence is forty, which is an enough value for a not-complicated shapes at present. Two base points in radius vectors may be possible, the center of gravity is a usual one and another is a mid-point of the length in the shape.

Forty pebbles from a riverside are prepared as solid samples. Their shapes are

Table 1. Dimension of pebble samples.

No.	Vol. [cc]	Area [cm^2]	Bulkiness [mm] Length	Breadth	Thick.	L.B.T. [cc]	L.B.T/Vol. [-]
1	13.5	31.2	48.0	29.0	18.5	25.8	1.91
2	15.5	33.7	48.5	34.0	18.5	31.5	1.97
3	11.2	28.5	44.0	25.0	18.0	19.8	1.77
4	11.0	28.1	37.5	33.5	16.0	20.1	1.83
5	11.1	26.3	39.0	26.5	20.0	20.7	1.86
6	7.5	21.1	41.0	22.5	15.0	13.8	1.84
7	24.5	50.4	68.0	33.0	20.0	44.9	1.83
8	7.9	19.8	37.5	21.0	15.0	11.8	1.50
9	13.0	34.8	52.5	32.5	16.5	28.2	2.17
10	19.5	40.7	54.0	30.0	21.0	34.0	1.74
11	9.0	26.4	41.0	31.0	13.0	16.5	1.84
12	10.0	25.7	36.0	27.5	15.0	14.8	1.48
13	8.0	22.6	36.0	28.0	15.0	15.1	1.89
14	19.0	40.8	59.5	28.0	20.5	34.2	1.80
15	10.5	30.1	41.0	36.0	14.5	21.4	2.04
16	5.7	19.6	35.5	25.5	10.0	9.0_5	1.59
17	8.9	23.0	37.5	25.0	16.0	15.0	1.68
18	8.3	24.5	44.0	25.0	15.0	16.5	1.99
19	12.5	30.2	41.5	32.5	18.0	24.3	1.94
20	19.0	32.8	51.5	29.0	24.0	35.8	1.89
22	19.0	40.3	48.0	29.5	20.0	28.3	1.49
23	7.8	20.0	31.0	23.0	19.0	13.6	1.74
25	10.0	27.2	42.5	29.5	17.0	21.3	2.13
26	8.6	21.8	39.5	20.5	18.0	14.6	1.70
27	16.0	38.8	45.0	49.0	19.5	43.0	2.69
28	8.9	23.9	41.0	29.0	15.0	17.8	2.00
29	11.0	26.2	39.5	24.5	23.0	22.3	2.02
30	19.0	40.3	42.5	35.5	29.0	43.8	2.30
31	12.0	32.1	61.0	25.0	17.5	26.7	2.22
32	8.9	22.1	33.0	28.0	19.5	18.0	2.02
33	16.5	38.0	52.5	34.5	18.5	33.5	2.03
34	16.0	38.1	47.5	38.0	18.5	33.4	2.09
37	17.5	35.5	39.5	36.0	27.0	38.4	2.19
42	6.2	19.8	37.0	22.5	14.5	12.1	1.95
45	19.0	44.5	55.0	45.5	15.5	38.8	2.04
46	14.0	34.7	48.5	34.5	17.5	29.3	2.09
47	13.5	36.9	50.0	28.0	25.5	35.7	2.64
50	8.0	20.4	31.5	28.0	14.5	12.8	1.60
51	15.0	41.6	50.0	48.5	11.5	27.9	1.86
52	17.0	37.7	54.5	33.0	15.5	27.9	1.64

not-rugose and not-concave and they satisfy our simplified requirements. Basic dimensions such as surface areas, volumes and bulkiness ratio are listed in Table 1. As usual, surface area of the body is grated by many pieces of section paper and these are accumulated as the area. Their volumes are displacement of water volume and bulkiness is determined from the Feret's boxing.

Experimental procedures are as follows;

1. *Rocation of a sample body.* Apparent maximum projection of the solid, on which a stick for clamping is glued along the extension of its length, is settled to direct to an initial view as a stable allocation (Fig. 10),

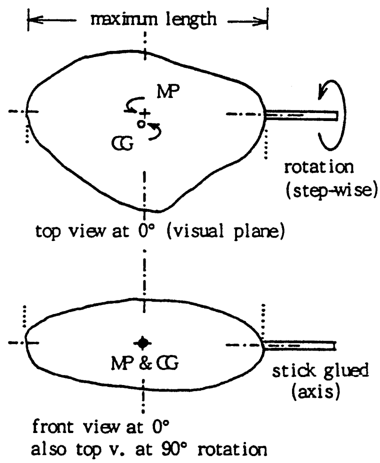

Fig. 10. Sample setting and a selection of a base point. CG: center of gravity, MP: middle point of the maximum length (or of Feret's diameter).

2. *Images of the body.* Silhouette are monitored into the analyser and the procedure are iterated by several incremental rotations equally spaced about only a horizontal angle,

3. *Radius vectors, $f(t)$ from the silhouettes.* They are sampled on the two base points and transformed by the Fourier method (half-range),

4. *Fourier coefficient.* The sine coefficient is mainly treated numerically because of better convergency than the cosine coefficient.

For the visual purpose, shape alternation according to the rotation about the axes are illustrated in Fig. 11.

Figure 12 is a usual relation with a 2/3-power between the actual areas and the corresponding volumes of pebbles.

4. ANALYSIS

The above two basis points, the center of gravity (two-dimensional) and the mid-point may affect on radius vector of plane figures in slightly different ways. In three-dimensional problems, the center of gravity is shifted according to the change

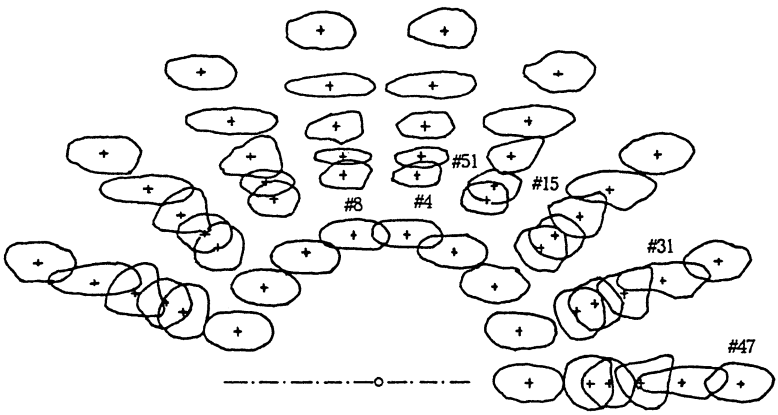

Fig. 11. Sketch of silhouettes of a sample of pebbles in incremental rotation.

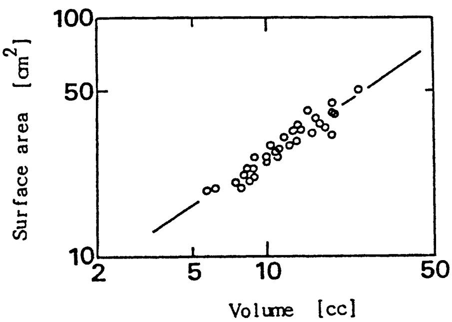

Fig. 12. Original data (pebbles). Relation between surface area and volume.

of view sides or directions in spite of its soundness of dynamics. On the other hand, the mid-point (middle point) keeps the same position, which is one of preferable properties, if the axis of rotation is deflect-free. In order to confirm the substitution of base point, two sets of the sine coefficients for a somewhat characteristic shape are presented in Fig. 13. There is a few disagreement in higher harmonics but it is considered to be not-troubled in lower ones. In the following, the mid-point is chiefly selected as the point.

Then, the estimation method of surface area and volume in terms of the Fourier coefficients are discussed. Figure 14 is an introductive relation between the measured surface area and the estimated area where a dimensional characteristic squared, $B(k, \theta)^2$ are summed up for forty points (Fourier samples) by 18 frames (10 step-deg. half-rotation) in the manner as Parseval's theory. No substantial differences in correlation coefficients between the two base points may permit us to use the mid-point as the base. Figure 15 is a case of a volume estimation as well as Fig. 14. In comparison of the area estimation to the volume, we found that the flatter shape has a tendency to inferior accuracy similar as in two dimensional classifications.

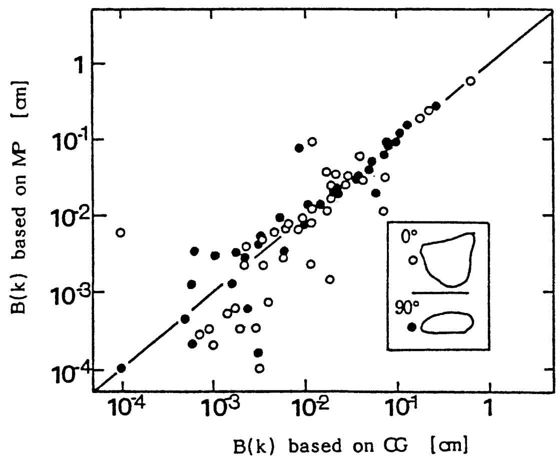

Fig. 13. Comparison of Fourier sine coefficients according to different base points (origin). CG: center of gravity, MP: middle point of Feret's diameter.

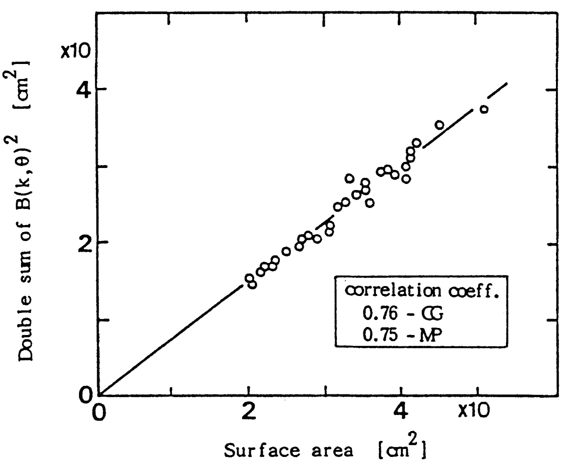

Fig. 14. Surface area of pebbles—Two origins (center of gravity, CG and middle point of Feret's diameter, MP) show almost same results for surface area estimation via radius vectors—.

Modification by a three dimensional flatness defined by next f will mitigate the scattered data (based on the mid-point) as Fig. 16.

$$f = \Sigma_k \log(B(4k+1)/B(4k+3))_{\theta=0} / \Sigma_k \log(B(4k+1)/B(4k+3))_{\theta=90} \quad (9)$$

4.1 Effects of the incremental angle-step for rotation of the bodies on the surface and volume estimations

As above mentioned, the solid body were rotated by steps of 10 degs. The step size should be adjusted according to complexity of surface states. However, in the

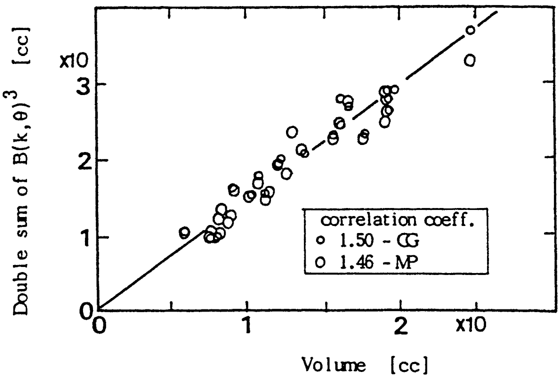

Fig. 15. Volume of pebbles.

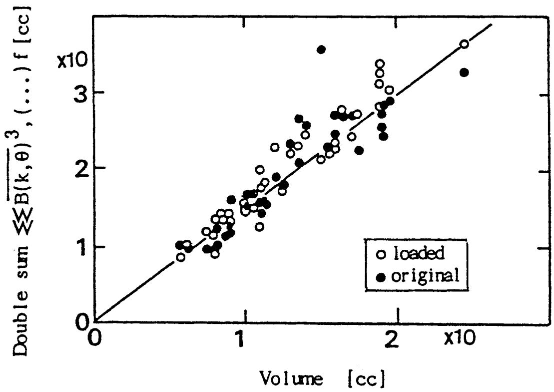

Fig. 16. Flatness-factor loading for volume estimation.

statistical view, we want to use a larger step-angle under the stable estimations, if possible. Figure 17 includes two cases of projections. One is the single projection without the rotation and it is the extreme shown by a key "o". Previous groups of particles have been measured to determine the plane size in this way. Such size is strongly affected by the orientation or the allocation of solid bodies and flat or longer shapes are apts to be estimated larger sizes. On the other side, the estimated surface area by multiple-projections show more narrower scattering of the data, a small effect of the step size of rotations and lower values than the single-projection, because of additional viewing of smaller project-planes (the second side). A ratio of the actual surface area to its mean projected area in the present case is 3.46 which is less than the Cauchy factor of 4.0 (Vouk, 1948) from Figs. 17 & 18. The reason why we have observed the smaller value is the omission of the third rotation based on the breadth (the shortest diameter). In spite of this, the surface areas of various irregular shape put in a good order along the line. Therefore, it is concluded that the method is available to estimate the surface area.

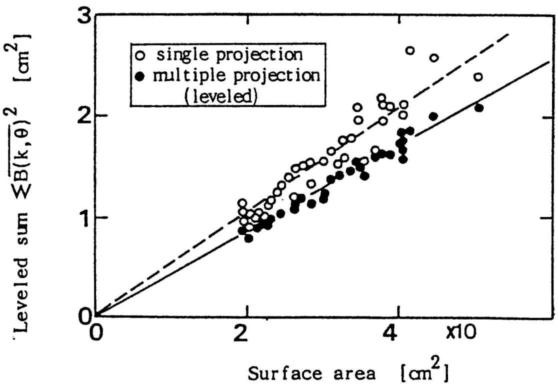

Fig. 17. Effect of angle-increment for projection on surface area estimation (leveled).

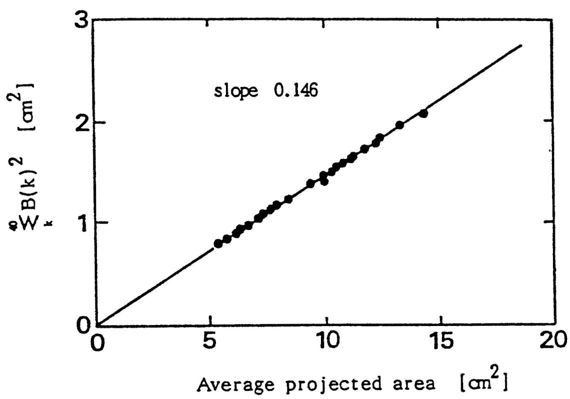

Fig. 18. Relation between average projected area (plane) and sum of $B(k)^2$.

Effects of the incremental angles on the volume estimation are shown in Fig. 19. The coarse steps such as the single or double frames are insufficient apparently, but more projections than three show a close and available result for the indirect estimation of the solid volume.

In addition to systematic projections, several random or skipped selections of planes from regular incremental angle will be interesting especially in the complicated situations. A coarse incremental angle of 60-deg., i.e. three frames shows almost stable both for the volume and surface area estimations and a smaller than 30-deg. will be not necessary (Fig. 20). Here, Data with a key "●" are results from three and five random samples among the 10-deg. samples. It is remarkable that the random sets are also useful. The number of Fourier coefficients, forty is not so large, but for more faster or not-precise guess, some cut-off of coefficient terms is possible as shown in Fig. 21.

As mentioned above, the surface area has been estimated by the Fourier analysis in the limited condition where a solid body is not concave and the volume

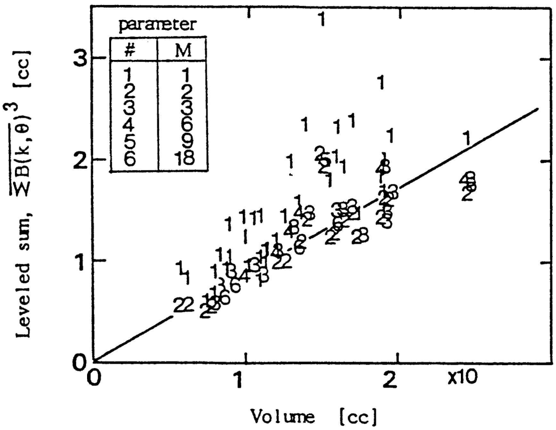

Fig. 19. Effect of angle-increment for projection $\overline{B(k, \theta)}^3 = \sum_m \sum_k |B(k, m\pi/M)^3|/M$.

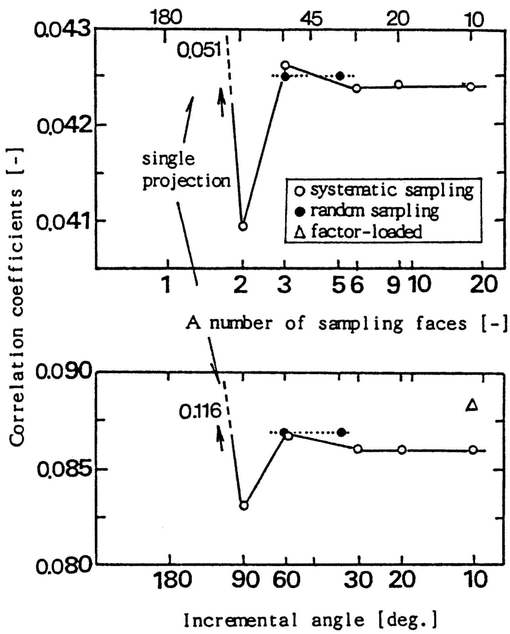

Fig. 20. Stability of correlations or measurements. above: surface area, below: volume.

was apted to show a some characteristic indication by shape parameters such as the elongation. Unless one does not mind any complication, the Fourier descriptors (of three dimensions) are useful for building up the classification indexes. For example, a sum, alternate from odd sine coefficients, $F1$, defined by

$$F1 = \Sigma_{\text{deg}} \Sigma_k \log |B(\text{deg}, 2k + 1)/B(\text{deg}, 2k + 3)| \qquad (10)$$

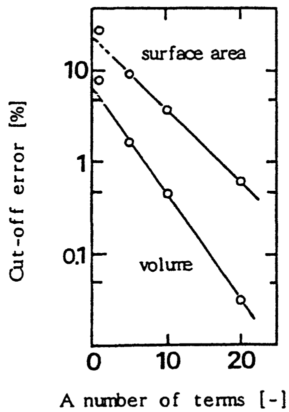

Fig. 21. Cut-off errors in estimation of surface area and volume (whole coeffs. −40).

is a measure of 3D rodness (or elongation).

A ratio of the coefficients with same harmonics but different incremental-angle, $F2$ renders larger irregularity

$$F2 = \Sigma_{\text{deg}} \Sigma_k \log |B(\text{deg}, 2k + 1)/B(\text{deg}', 2k + 1)|. \tag{11}$$

3D flatness is determined with $F3$ defined by

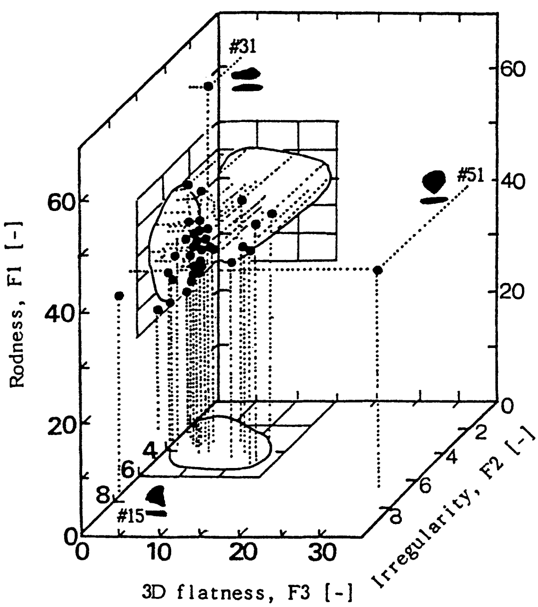

Fig. 22. Shape distribution of pebbles in a characteristic space.

$$F3 = \Sigma_{\text{deg}} \log |SB(\text{deg})/SB_{\text{av}}| \quad (12)$$

$$SB(\text{deg}) = \Sigma_k |B(\text{deg}, 2k+1) - B(\text{deg}, 2k+3)| \quad (13)$$

$$SB_{\text{av}} = \Sigma_{\text{deg}} SB(\text{deg})/\text{number of planes (or frames)}. \quad (14)$$

Into a coordinate space with the above three indexes, we can set the sample pebbles in a characteristic way as in Fig. 22. These classification will be forward to further 3D-analyses.

SUMMARY

First, a discrete Fourier transformation method (half-range) is examined. Some of the sine coefficients can be related through geometrical informations.

Next, multiple projections of pebble samples are developed to surface area and volume of the pebble through the discrete sine coefficients.

REFERENCES

Ahmed, N., Natarajan, T., and Rao, K. R. (1974): Discrete cosine transform, *IEEE Trans. Comput.*, C**23**, 90–93.

Beddow, J. K. and Philip, G. (1975): On the use of a Fourier analysis technique for describing the shape of individual particles, *Planseeber*, **23**, 3–14.

Ehrlich, R. and Weinberg, B. (1970): An exact method for characterizing grain shape, *J. Sediment. Petrol.*, **40**, 205–212.

Jain, A. K. (1979): A sinusoidal family of unitary transforms, *IEEE Trans. on Patt. Anal. & Machine Intell.*, PAMI-1, 356–365.

Luerkens, D. W., Beddow, J. K., and Vetter, A. F. (1982a): Morphological Fourier descriptors, *Powder Technol.*, **31**, 209–215.

Luerkens, D. W., Beddow, J. K., and Vetter, A. F. (1982b): A generalized method of morphological analysis (the (RS) method), *Powder Technol.*, **31**, 217–220.

Meloy, T. P. (1977): A hypothesis for morphological characterization of particle shape and physico-chemical properties, *Powder Technol.*, **16**, 233–253.

Oppenheim, A. V. and Lim, J. S. (1981): The importance of phase in signals, *Proc. IEEE*, **69**, 529–541.

Schwalcz, H. P. and Shane, K. C. (1969): Measurement of particle shape by Fourier analysis, *Sedimentology*, **13**, 213–231.

Shanmugam, K. S. (1975): Comments on 'Discrete cosine transform', *IEEE Trans. Comput.*, C**24**, 759.

Vouk, V. (1948): Projected area of convex bodies, *Nature*, **162**, 330–331.

Zahn, C. T. and Roskies, Z. T. (1972): Fourier descriptors for plane closed curves, *IEEE Trans. Comput.*, C**21**, 269–281.

DISCUSSION

Q. A particle of any shape can be expressed in terms of expansion by the spherical harmonic function. Is it possible to calculate their coefficients from the data obtained by your method? (Takaki, R.)

A. We are not sure at this point, however, the spherical harmonics with half integers are also definable and they may be very inclusive.

C. As I understand it, the only totally unbiased way of estimating specific particle surface is by the use of lower dimensional (i.e. linear) probes. Your discrete Fourier Sine transformation would certainly be sensitive to departures from convexity. There is an interesting paper by Baddeley *et al.* (1986, *J. Microscopy* **142**: 259–276) which describes a technique that will allow you to unbiasedly estimate the surface of specific particles using sine weighted linear probes, for direct comparison of the results obtained by your method. (Howard, C. V.)

Thank you for the information we were not aware of. Surely, Baddeley, Gundersen & Cruz-Orive discussed the surface area under the title of "Estimation of Surface Area from Vertical Section".

Our method uses several vertical surface projections (and Fourier transformation) and this should be distinguished methodologically, from the vertical sectioning by cutting the body.